NIH Public Access
Author Manuscript
*Appl Spectrosc*. Author manuscript; available in PMC 2015 October 01.

Published in final edited form as:
*Appl Spectrosc*. 2014 ; 68(10): 1168–1175. doi:10.1366/13-07327.

# The contribution of bone and cartilage to the near-infrared spectrum of osteochondral tissue

**Cushla M. McGoverin**[a], **Karl Lewis**[a,b], **Xu Yang**[c], **Mathias P. G. Bostrom**[c], and **Nancy Pleshko**[a,c,*]

[a]Department of Bioengineering, College of Engineering, Temple University, 1947 North 12th St., Philadelphia, PA 19122

[c]Research Division, Hospital for Special Surgery, 535 East 70th St., New York, NY 10021

## Abstract

Near-infrared (NIR) spectroscopy has been utilized to assess hyaline cartilage quality in human and animal osteochondral tissues. However, due to the lack of NIR signal from bone phosphate, and the relatively deep penetration depth of the radiation, the separate contributions of cartilage and bone to the spectral signatures have not been well defined. The objectives of the current study were 1) to improve the understanding of the contributions of bone and cartilage to NIR spectra acquired from osteochondral tissue, and 2) to assess the ability of this non-destructive method to predict cartilage thickness and modified Mankin grade of human tibial plateau articular cartilage. NIR spectra were acquired from samples of bovine bone and cartilage with varying thicknesses, and from twenty-two tibial plateaus harvested from patients undergoing knee replacement surgery. Spectra were recorded from regions of the tibial plateaus with varying degrees of degradation, and the cartilage thickness and modified Mankin grade of these regions were assessed histologically. Spectra from bone and cartilage samples of known thicknesses were investigated to identify spectral regions that were distinct for these two tissues. Univariate and multivariate linear regression methods were used to correlate modified Mankin grade and cartilage thickness with NIR spectral changes. The ratio of the NIR absorbances associated with water at 5270 and 7085 $cm^{-1}$ were the best differentiator of cartilage and bone spectra. NIR prediction models for thickness and Mankin grade calculated using partial least squares regression were more accurate than univariate-based prediction models, with root mean square errors of cross validation of 0.42 mm (thickness) and 1.3 (modified Mankin grade), respectively. We conclude that NIR spectroscopy may be used to simultaneously assess articular cartilage thickness and modified Mankin grade, based in part on differences in spectral contributions from bone and cartilage.

### Keywords

osteoarthritis; partial least squares regression; near-infrared spectroscopy; bone; cartilage

[*]Corresponding Author: Nancy Pleshko, PhD, Department of Bioengineering, College of Engineering, Temple University, 1947 North 12th St., Philadelphia, PA 19122, Phone: 215-204-4280, npleshko@temple.edu.
[b]Current address: Department of Biomedical Engineering, City College of New York, 160 Convent Avenue, New York, NY 10031

NIH-PA Author Manuscript
NIH-PA Author Manuscript
NIH-PA Author Manuscript

NIH-PA Author Manuscript

NIH-PA Author Manuscript

NIH-PA Author Manuscript

## Introduction

Clinical osteoarthritis (OA) has a large and increasing prevalence in the United States. Twenty one million people over 25 years old were estimated to have OA in 2001 (7% of the 2001 US population[1]), and 26.9 million people in 2008 (9% of the 2008 US population[1]).[2] Estimates of OA affliction are expected to continue to grow as age and obesity increase within the population.[2–6] Osteoarthritis may be debilitating and in later stages may only be effectively treated by replacing the damaged joint. In the 65–74 year old age category OA is the fifth most common reason for disability.[7] Reduction or reversal of OA progression in the initial stages of development would be the optimal treatment option.

Current methods for diagnosing OA include arthroscopy, radiography and magnetic resonance imaging (MRI).[8–11] Arthroscopy, a minimally invasive technique, provides visual information for assessing OA development, including the color and texture of articular cartilage (AC).[12,13] Radiography informs about joint space narrowing, joint space width, subchondral sclerosis, marginal osteophytes and malalignment.[14–16] Magnetic resonance imaging (MRI) provides similar information to radiography, although the three dimensional perspective allows for a better overview of the joint space.[17, 18] In addition, all tissues involved in OA (cartilage, bone, menisci) are observable using MRI. Advanced OA may be identified by any of these three methods; however, early stage OA is more difficult to diagnose with physical techniques.[19, 20]

The matrix composition of articular cartilage changes throughout the onset and development of OA. During the development of OA the collagen network of articular cartilage is disrupted, water content increases and proteoglycan content decreases, resulting in a loss of mechanical stress resistance.[20, 21] Histology, biochemistry and gravimetrics (water assessment) have been used to identify subtle compositional changes of articular cartilage during the onset of OA in animal models.[22] Histologically, Mankin grading,[22] and OARSI grading[23, 24] are two grading systems that are widely used to assess severity of tissue degradation. While these techniques are informative and sometimes precise, they require harvesting and destruction of the tissues of interest, and thus are typically only utilized in pre-clinical studies. An ideal early diagnosis method would provide data on tissue status using a rapid and non-destructive, minimally (or non-) invasive analyses.

Infrared (IR) spectroscopy, a technique based on the absorption of radiation that causes molecular vibrations, has been used to assess organic materials, and has proven to be useful in studies of OA.[25–31] Both mid-IR spectroscopy (frequency range 400–4000 $cm^{-1}$) and near-IR (NIR) spectroscopy (frequency range 4000–13,000 $cm^{-1}$) have been utilized to assess cartilage degradation.[25–28, 30–32] Mid-IR spectra are characterized by relatively sharp peaks that may be attributed to specific chemical functionality within the molecules of the sample, and the spectra for bone and cartilage are very well defined.[25, 33] In contrast, NIR spectra are characterized by broad and overlapping peaks that are mostly attributed to C–H, N–H and O–H chemical functionality, and have only recently had specific molecular species assigned to features in cartilage spectra.[31, 34, 35] Interestingly, there is no NIR signal from the phosphate molecules in bone, whereas in the mid-IR region, the phosphate absorbance is one of the largest. However, NIR spectroscopy has the distinct advantage of penetrating to a

NIH-PA Author Manuscript

NIH-PA Author Manuscript

NIH-PA Author Manuscript

greater sample depth (mm to cm) compared to mid-IR spectroscopy.[36–38] Non-destructive mid-IR analyses are confined to the surface of samples, and a maximum depth on the order of ~2 μm is interrogated when using attenuated total reflectance (ATR) mid-IR spectroscopy. [36]

Near-IR spectroscopy has previously proven to be useful for studying articular cartilage degradation,[28–31, 35, 39–44] including in a surgical environment.[28–31] Importantly, a significant correlation has been found between the International Cartilage Repair Society (ICRS) grading of cartilage and a ratio of peak areas in a NIR spectrum of cartilage.[31, 35] Furthermore, partial least squares regression (PLSR) has been used to correlate NIR spectra of bovine articular cartilage with thickness,[40] and NIR spectra of rat articular cartilage with thickness,[39] Mankin grade,[39] subchondral bone volume[41] and mineral density.[41] The spectral basis for these correlations has not been well defined, particularly with respect to the contribution of subchondral bone. In the current study, we investigated NIR spectral contributions from bone and cartilage, and demonstrated that PLSR can be used to predict modified Mankin grade and thickness of human knee articular cartilage from NIR spectral data.

## Materials and methods

### Tissues

**Human tissues—**Twenty two tibial plateaus from male and female patients undergoing knee replacement surgery (ages 46–87) were harvested with institutional (Hospital for Special Surgery, New York, USA) IRB approval. Harvested tibial plateaus were removed from the operating room and taken immediately to an adjacent laboratory for infrared spectroscopic data collection. Tissues were kept moist during data collection, and synovial fluid was cleaned from the cartilage surface with 0.9% saline.

**Bovine Tissues—**Bovine nasal cartilage (BNC), articular cartilage, and bone (supplied by JBS, Souderton, PA, and by Research 87, Boylston, MA) were used for characterizing the depth of NIR penetration, and for characterizing the NIR spectrum of cartilage and bone. For the depth penetration studies, 14 sections of BNC were prepared, ranging in thickness from 0.37 to 5.45 mm. BNC is a hyaline cartilage that has a more homogeneous composition compared to articular cartilage, and thus was used for assessment of penetration to minimize compositional differences as a confounding factor. Each BNC section was mounted on a non-reflective surface for NIR data collection (three spectra for each section). The non-reflective surface was then lined with parafilm and a second set of NIR spectra were collected. Parafilm has a unique peak at 5774 $cm^{-1}$ that was used to assess depth of penetration.

Bovine articular cartilage and bone samples were harvested from a 2–3 week old bovine stifle joint using a 5 mm diameter biopsy punch. The bone and cartilage of the punched sample were separated and NIR spectra were recorded from each tissue. Five samples that were approximately 5 mm thick total but contained different amounts of bone and cartilage were generated for assessment of the underlying bone contribution to the cartilage spectra; the ratio of bone to cartilage thickness ranged from 0.2 to 2.7.

NIH-PA Author Manuscript

NIH-PA Author Manuscript

NIH-PA Author Manuscript

### Near-infrared spectroscopy

Diffuse reflectance NIR spectroscopy was performed using a Remspec NIR probe (Charlton, MA) coupled to a matrix-F spectrometer (Bruker Optics, Billerica, MA). Data were collected with OPUS version 5.5 (Bruker Optik GmbH, Ettlingen, Germany). The probe was placed in contact with the cartilage or bone surface. Spectra were the sum of 32 co-added scans across the spectral range of 12,000–4000 $cm^{-1}$ with a spectral resolution of 16 $cm^{-1}$. Background spectra of air were collected with a mirror before each series of measurements.

Several regions were sampled from each tibial plateau (medial and lateral) and three spectra were collected from each region. A total of 35 sampling sites were identified for a total of 105 spectra. Triplicate spectra were also collected from each BNC section (with and without parafilm beneath) and from the bovine articular cartilage and bone samples. Bovine nasal and articular cartilage, and bone samples were placed on a non-reflective background when spectra were collected.

### Histology

The 35 tibial plateau regions that were evaluated spectroscopically were also sectioned for histology. The cartilage and subchondral bone were removed from each region (that had been spectroscopically sampled) with a 5 mm diameter biopsy punch, and then immersed in a mixture of 80% ethanol and 1% cetylpyridinium chloride. The samples were subsequently decalcified in a 10% EDTA/Tris buffer solution, embedded in paraffin and sectioned to a thickness of 7 μm onto glass slides. These sections were stained with safarin-O, hematoxylin and eosin, and graded according to a modified Mankin scale.[45] The Mankin grading system is a standard for the assessment of cartilage and incorporates grading based on structure fissuring, cell cloning, loss of proteoglycans, and tidemark integrity. In the modified scale, a grade of 0 represents normal cartilage and a grade of 13 represents severely degenerated cartilage (Table I).[46, 47] Two investigators independently evaluated samples that had been blind-coded and randomized. The average of these two grades was used as the final modified Mankin grade. The Cohen's Kappa index was calculated using the 'wkappa' function (psych package version 1.2.4)[48] in R version 2.15.2[49] to assess the level of agreement between the two investigators. The thickness of cartilage was measured from the histology images using Image J version 1.45s;[50] the lengthes of ten lines drawn from the cartilage surface to the bone spanning the width (~5 mm) of the section were averaged.

### Data analysis

Spectral preprocessing, principal component analysis (PCA) and partial least squares regression (PLSR) were performed with Unscrambler X (CAMO Inc, Norway), and peak integrations were performed in OPUS version 5.5. PCA was used to identify spectral outliers in the tibial plateau dataset; two outlying spectra were identified in the principal component one (PC1) versus PC2 scores plot. Visual inspection of the raw data indicated these spectra had a low signal to noise level and were subsequently removed from the dataset. Spectra from each tibial plateau region were truncated to 11,000–4000 $cm^{-1}$, averaged and baseline offset corrected, prior to the calculation of absorbance areas in the following spectral regions: 8820–8060, 8695–8197, 7460–6780, 7280–6040, 5716–5496 $cm^{-1}$. Relationships between the integrated band intensities or ratios thereof (8820–8060/5716–5496, 7460–

NIH-PA Author Manuscript

NIH-PA Author Manuscript

NIH-PA Author Manuscript

6780/8695–8197, 7280–6040/8820–8060, 7280–6040/5716–5496) and modified Mankin grade or thickness, were evaluated using Spearman correlation with a $P < 0.05$ level of significance. The integrated bands were attributed to CH stretching second overtones associated with matrix components (8820–8060 and 8695–8197 $cm^{-1}$), OH stretching first overtones primarily associated with water (7460–6780 and 7280–6040 $cm^{-1}$) and CH stretching first overtones (5716–5496 $cm^{-1}$).[51] The two spectral regions, 8695–8197 and 7280–6040 $cm^{-1}$ were integrated for direct comparison to the study of Spahn et al.[35] The height of five peaks (8640, 8266, 6418, 6025, 5824 $cm^{-1}$) were evaluated in spectra that were preprocessed from 11,000–4000 $cm^{-1}$ using standard normal variate (SNV) and Savitzky-Golay second derivatives (third order polynomial, 339 $cm^{-1}$ window: 2dSG3,339). These peaks were attributed to CH stretching second overtones (8640 and 8266 $cm^{-1}$), NH stretching first overtones (6418 $cm^{-1}$) and CH stretching first overtones (6025 and 5824 $cm^{-1}$).[51] In addition, the minimum peak height in the spectral ranges 8660–8600, 7100–7040 and 5290–5240 $cm^{-1}$ and the wavenumber of this minimum peak height were investigated. Ratios of these minimum peaks heights were calculated: 5290–5240/7100–7040, 5290–5240/8660–8600 and 7100–7040/8660–8600 $cm^{-1}$. The relationships between these peak heights and ratios with thickness or modified Mankin grade were tested using Spearman correlation with a 0.05 level of significance.

PLSR prediction models for modified Mankin grade and cartilage thickness were calculated using the 9000–4400 $cm^{-1}$ spectral region. These spectral data were preprocessed using the standard normal variate transform followed by calculating the Savitzky-Golay (SG) second derivatives (third order polynomial) using one of three window widths: 170, 255 and 339 $cm^{-1}$. Large window widths were required for second derivative preprocessing to adequately smooth the NIR data. Mean centering was applied prior to all PLSR calculations.

Modified Mankin grading and cartilage thickness were analysed with PLSR, a multivariate linear regression method based on the calculation of latent variables which represent the maximum covariance between the X (spectral) and Y (modified Mankin grade or cartilage thickness) matrices.[52] PLSR prediction models were validated using an eight segment cross validation procedure; samples were randomly assigned to each segment. Outlying samples were identified using Hotelling $T^2$ residuals; these spectra were further investigated. Prediction models were evaluated on the basis of the number of factors required, coefficient of correlation of calibration and cross validation and root mean square error of calibration and cross validation (RMSEC and RMSECV respectively; equation 1).

$$RMSE = \sqrt{\frac{\sum_{i=1}^{i=N} (Y_{i,Predicted} - Y_{i,Measured})^2}{N}} \quad \text{Equation 1}$$

where N is the number of samples.

NIH-PA Author Manuscript

NIH-PA Author Manuscript

NIH-PA Author Manuscript

# Results

## Sample characteristics

The averaged modified Mankin grades of the dataset ranged from 2 to 11, with a median of 6.5. The difference between the two investigators' grades ranged from 0 to 3, the mean difference was 1. The inter-rater agreement was moderate as the linearly weighted kappa value was 0.6.[53] Cartilage thickness of the samples ranged from 0.95 to 3.68 mm with an average of 2.35 mm (standard deviation 0.65 mm). Within a sample the smallest relative standard deviation (RSD) of cartilage thickness was 0.82% and the largest was 30.33%, the average sample RSD was 9.34%.

## NIR penetration depth into cartilage

The unique parafilm peak at 5774 $cm^{-1}$ was readily apparent in the second derivative of the NIR spectrum (Fig. 1). The intensity of this peak decreased with increasing thickness of the cartilage layer overlaying the parafilm section, and was not observed when samples were greater than 5 mm thick. Thus, the penetration depth of the NIR radiation was estimated to be under 5 mm in this spectral region.

## Features of cartilage NIR spectra

NIR spectra of cartilage were characterized by a broad absorption band in the range 5450–4300 $cm^{-1}$, a broad and intense peak around 7000 $cm^{-1}$, a broad and low intensity band around 8450 $cm^{-1}$, and minor peaks between 4300–4000 $cm^{-1}$, and between 6000–5450 $cm^{-1}$ (Fig. 2a). The band centered around 5200 $cm^{-1}$ has been attributed to a combination of 'free' water and bound water, while the absorption peak in the 7000 $cm^{-1}$ spectral region has been attributed to free water.[34] The NIR spectra of bone had absorbances in the same spectral regions as cartilage, however, the peaks were less broad than in cartilage. Peaks at 5270 and 7085 $cm^{-1}$ were particularly intense in second derivative-transformed spectra of cartilage, with lower intensity bands observed at 4675, 5624, 6653, and 8640 $cm^{-1}$ (Fig. 2b). Second-derivative transformed spectra of bone had low intensity peaks at 5624 and 8645, and dominant peaks at 5220 and 7050 $cm^{-1}$.

The ratio of these two bands informs about the ratio of bound and free water in a sample, and the 5270:7085 $cm^{-1}$ ratio was higher in bone when compared with cartilage (Fig. 2c). For samples with both cartilage and bone, the ratio of 5270 to 7085 $cm^{-1}$ increased as the ratio of bone thickness to cartilage thickness increased (samples in the studied series had the same total thickness). Several bands of changing intensity were also identified in the second derivative spectra of degraded cartilage samples (Fig. 3), including 8266, 6025 and 5824 $cm^{-1}$, which have been attributed to C-H stretching second and first overtones (cartilage sections, spectra and 2$^{nd}$ derivative spectra: Fig 3a, b, c, respectively).[51] Within bone spectra the bands around 5624 and 8645 $cm^{-1}$ arise from bone collagen, and the 5220 and 7085 $cm^{-1}$ are attributed to water.

Although there was a negative trend between modified Mankin grade and cartilage thickness, ($R = -0.24$), the correlation did not reach significance ($P = 0.20$). However, both cartilage thickness and modified Mankin grade were significantly correlated with several

NIH-PA Author Manuscript

NIH-PA Author Manuscript

NIH-PA Author Manuscript

peak areas and second derivative parameters. R values ranged from −0.57 to 0.66 for thickness and −0.56 to 0.61 for modified Mankin grade with respect to peak area parameters and −0.75 to 0.70 for thickness and −0.60 to 0.36 for modified Mankin grade with respect to second derivative peak height parameters (Table II).

The PLSR model for the prediction of cartilage thickness, using spectra pretreated with SNV and second derivative transformation (third order, 170 $cm^{-1}$ window), used three factors and had a calibration $R^2 = 0.75$, RMSEC = 0.32 mm, validation $R^2 = 0.61$ and RMSECV = 0.42 mm. The model for the prediction of modified Mankin grade, using spectra pretreated with SNV and second derivative transformation (third order, 339 $cm^{-1}$ window), used five factors and had a calibration $R^2 = 0.84$, RMSEC = 0.9, validation $R^2 = 0.64$ and RMSECV = 1.3. A large difference between RMSEC and RMSECV is indicative of an over-fit model, and a comparison of these parameters indicate that the models were not over-fit; the RMSECV was 70 and 80% of the RMSEC for modified Mankin grade and thickness respectively. The loading weights of the three factors of the cartilage thickness model were dominated by the 5300 and 7100 $cm^{-1}$ spectral regions (Fig. 4). In the modified Mankin grade model, in addition to the water absorbances, other lower wavenumber features attributable to matrix absorbances were also strong contributors to the loading weights.

## Discussion

Near-IR light penetrates up to 5 mm into a cartilage sample in the 5774 $cm^{-1}$ spectral region. Though the penetration depth will vary with respect to frequency (wavelength) with higher frequencies having a greater penetration depth it is likely the near infrared wavelengths used here interact with all four zones of articular cartilage from the superficial to the calcified cartilage zone, as well as the underlying subchondral bone. The spectra in our study are therefore informative about the chemical and physical composition of cartilage beyond the direct interface between the probe tip and the sample surface; cartilage in our study ranged in thickness from 0.95 to 3.68 mm. Furthermore, the articular cartilage in the medial condyle of a healthy human knee is 2.92 mm thick on average.[54] Hence, the diffuse reflectance spectra collected from each tibial plateau sampled the entire thickness of cartilage and interrogated the underlying subchondral bone. Although the penetration depth of NIR spectroscopy may offer a substantial advantage over the limited penetration of attenuated total internal reflection mid-IR spectroscopy, the NIR signal cannot directly separate the bone and cartilage contributions, and represents an average of the tissues being sampled.

Clinical osteoarthritis disrupts the extracellular matrix of articular cartilage, degrading the cartilage surface and reducing the cartilage thickness. Despite this known relationship, we did not recover a strong, significant correlation between cartilage thickness and modified Mankin grade. Instead, we observed substantial variation in the thickness of tibial plateau cartilage at different modified Mankin grades. Thus, cartilage thickness and modified Mankin grade may not correlate in patients with osteoarthritis. This is consistent with a previous study that showed substantial variation in the thickness of normal tibial plateau cartilage (average minimum = 0.35, $\sigma = 0.27$ mm; average maximum = 6.25 mm, $\sigma = 0.27$ mm; $n = 12$),[54] and highlights the patient to patient variation.

NIH-PA Author Manuscript

NIH-PA Author Manuscript

NIH-PA Author Manuscript

Nevertheless, correlations were sought between NIR spectral parameters and thickness or modified Mankin grade. Here, the spectral parameters of interest were peak areas calculated from baseline offset corrected spectra, and peak heights obtained from second derivative spectra. Modified Mankin grade was most strongly correlated ($R = 0.61$, $P < 0.05$) with a peak area ratio representing the ratio of water to organic matrix in the sample (7280–6040/8820–8060 $cm^{-1}$). This positive correlation tracks the increase in water content relative to proteoglycan and collagen content that occurs with OA. The correlation coefficient between modified Mankin grade and the peak area ratio of 7460–6780 to 8695–8197 $cm^{-1}$ ($R = 0.60$) was similar to a previous study based on ovine knee articular cartilage ($R = 0.69$).[35] Second derivative preprocessing was effective at resolving peaks within spectra of bone and cartilage. The strongest correlation between modified Mankin grade and second derivative spectral parameters involved the 7201–7000 $cm^{-1}$ region, i.e. the O-H stretching second overtone region that is largely associated with water. More specifically, the O-H stretching second overtone region increased in intensity as modified Mankin grade increased ($R = -0.60$; peaks have negative intensity in second derivative spectra).

Correlations were also sought between second derivative spectral parameters and cartilage thickness. The strongest correlations for thickness involved the C-H stretching second overtone region, 8755–8500 $cm^{-1}$. The peak intensity in the 8755–8500 $cm^{-1}$ region was more prominent in thicker cartilage samples, which have a proportionally higher organic component. Thickness correlations were found to be useful for assigning organic peaks in NIR spectra. With increased cartilage thickness the presence of a shoulder at 5824 $cm^{-1}$ was reduced, associating this particular C-H stretching first overtone with bone. Furthermore, the 8640 and 8266 $cm^{-1}$ peaks have elsewhere been attributed to C-H stretching second overtones,[51] and the opposing signs of the correlation coefficients indicate that the peaks are due to cartilage and bone respectively.

Prediction models for modified Mankin grade and thickness were calculated using the 4400–9000 $cm^{-1}$ spectral region and PLSR. The increased complexity of determining modified Mankin grade, compared to the relatively simple process of measuring cartilage thickness, likely accounts for the greater number of factors used in the modified Mankin grade prediction model. The 5200 and 7100 $cm^{-1}$ bands dominated the loading weights of all three factors of the thickness PLS prediction model; therefore, the spectral differences between bone and cartilage, based on differences in relative amount of bound and free water, formed the basis of the thickness calibration. However, modified Mankin grade predictions were based on more than just the spectral differences between bone and cartilage. Loading weights of the modified Mankin grade prediction model included bands associated with C-H and N-H functionality, and are likely due to changes in proteoglycan and collagen content and environment.

Our PLSR results compared favorably with other spectroscopic studies. For example, an earlier prediction of modified Mankin grade used mid-IR spectroscopy to study human tibial plateau articular cartilage (modified Mankin grades 2–10) and produced a prediction model with a root mean squared error of prediction (RMSEP) of 1.4.[45] Furthermore, a study of articular cartilage from rats coupled NIR spectroscopy and PLSR to predict modified Mankin grade (approximate range 5–13.5) and produced an RMSECV of 0.9 using leave-

NIH-PA Author Manuscript

NIH-PA Author Manuscript

NIH-PA Author Manuscript

one-out cross validation.[39] The thickness of bovine patellar cartilage was also studied with NIR spectroscopy: a PLSR prediction using the 8850–7200 $cm^{-1}$ spectral region produced an RMSEP of 0.07 mm from a cartilage thickness range of 1.20–2.42 mm.[40] The influence of thickness on cartilage spectra has also been investigated in the visible and short-wave NIR spectral region.[55–58] Intensities and RGB coordinates from visible images usefully predicted cartilage thickness below 1.5 mm (RMSEP 0.28 mm), although prediction efficacy was reduced for samples between 1.5 mm and less than 2.5 mm thick.[55]

In conclusion, near-IR spectroscopy may be used to simultaneously assess the thickness and modified Mankin grade of human tibial plateau articular cartilage. The NIR spectroscopic measurements presented here were performed *ex vivo*, however, this method could be adapted for *in vivo* analysis of arthroscopically accessible cartilage surfaces.

## Acknowledgments

This study was funded by NIH EB000744 and AR056145. Karl Lewis was funded by a NIH 34GM087239 Temple University MARC U-STAR training grant.

## References

1. United States Census Bureau. [accessed May 14 2013] http://www.census.gov/popest/data/historical/2000s/vintage_2008/index.html
2. Lawrence RC, Felson DT, Helmick CG, Arnold LM, Choi H, Deyo RA, Gabriel S, Hirsch R, Hochberg MC, Hunder GG, Jordan JM, Katz JN, Kremers HM, Wolfe F, Natl Arthritis Data W. Estimates of the prevalence of arthritis and other rheumatic conditions in the United States. Arthritis Rheum. 2008; 58(1):26–35. [PubMed: 18163497]
3. Moskowitz RW. The burden of osteoarthritis: clinical and quality-of-life issues. Am J Manag Care. 2009; 15(8 Suppl):S223–229. [PubMed: 19817508]
4. Kadam UT, Jordan K, Croft PR. Clinical comorbidity in patients with osteoarthritis: a case-control study of general practice consulters in England and Wales. Ann Rheum Dis. 2004; 63(4):408–414. [PubMed: 15020335]
5. Wang YF, Beydoun MA, Liang L, Caballero B, Kumanyika SK. Will all Americans become overweight or obese? Estimating the progression and cost of the US obesity epidemic. Obesity. 2008; 16(10):2323–2330. [PubMed: 18719634]
6. United States Census Bureau. [accessed May 14 2013] http://www.census.gov/population/projections/data/national/2012/summarytables.html
7. Michaud CM, McKenna MT, Begg S, Tomijima N, Majmudar M, Bulzacchelli MT, Ebrahim S, Ezzati M, Salomon JA, Kreiser JG, Hogan M, Murray CJ. The burden of disease and injury in the United States 1996. Popul Health Metr. 2006; 4:11. [PubMed: 17049081]
8. Friemert B, Oberlander Y, Schwarz W, Haberle HJ, Bahren W, Gerngross H, Danz B. Diagnosis of chondral lesions of the knee joint: can MRI replace arthroscopy? A prospective study. Knee Surg Sports Tr A. 2004; 12(1):58–64.
9. Brismar BH, Wredmark T, Movin T, Leandersson J, Svensson O. Observer reliability in the arthroscopic classification of osteoarthritis of the knee. J Bone Joint Surg Br. 2002; 84B:42–47. [PubMed: 11837831]
10. Blackburn WD, Chivers S, Bernreuter W. Cartilage imaging in osteoarthritis. Semin Arthritis Rheum. 1996; 25(4):273–281. [PubMed: 8834015]
11. Buckland-Wright C. Current status of imaging procedures in the diagnosis, prognosis and monitoring of osteoarthritis. Baillieres Clin Rheumatol. 1997; 11(4):727–748. [PubMed: 9429734]
12. Acebes C, Roman-Blas JA, Delgado-Baeza E, Palacios I, Herrero-Beaumont G. Correlation between arthroscopic and histopathological grading systems of articular cartilage lesions in knee osteoarthritis. Osteoarthr Cartilage. 2009; 17(2):205–212.

NIH-PA Author Manuscript NIH-PA Author Manuscript NIH-PA Author Manuscript

13. Pessis E, Drape JL, Ravaud P, Chevrot A, Dougados M, Ayral X. Assessment of progression in knee osteoarthritis: results of a 1 year study comparing arthroscopy and MRI. Osteoarthr Cartilage. 2003; 11(5):361–369.
14. Kellgren JH, Lawrence JS. Radiological assessment of osteo-arthrosis. Ann Rheum Dis. 1957; 16(4):494–502. [PubMed: 13498604]
15. Altman RD, Fries JF, Bloch DA, Carstens J, Cooke D, Genant H, Gofton P, Groth H, McShane DJ, Murphy WA, Sharp JT, Spitz P, Williams CA, Wolfe F. Radiographic assessment of progression in osteoarthritis. Arthritis Rheum. 1987; 30(11):1214–1225. [PubMed: 3689459]
16. Altman RD, Gold GE. Atlas of individual radiographic features in osteoarthritis, revised. Osteoarthr Cartilage. 2007; 15:A1–A56.
17. Menashe L, Hirko K, Losina E, Kloppenburg M, Zhang W, Li L, Hunter DJ. The diagnostic performance of MRI in osteoarthritis: a systematic review and meta-analysis. Osteoarthr Cartilage. 2012; 20(1):13–21.
18. Eckstein F, Cicuttini F, Raynauld JP, Waterton JC, Peterfy C. Magnetic resonance imaging (MRI) of articular cartilage in knee osteoarthritis (OA): morphological assessment. Osteoarthr Cartilage. 2006; 14:A46–A75.
19. Pollard TCB, Gwilym SE, Carr AJ. The assessment of early osteoarthritis. J Bone Joint Surg Br. 2008; 90B(4):411–421. [PubMed: 18378911]
20. Lorenz H, Richter W. Osteoarthritis: Cellular and molecular changes in degenerating cartilage. Prog Histochem Cytochem. 2006; 40(3):135–163. [PubMed: 16759941]
21. Venn M, Maroudas A. Chemical composition and swelling of normal and osteoarthrotic femoral-head cartilage .1. Chemical composition. Ann Rheum Dis. 1977; 36(2):121–129. [PubMed: 856064]
22. Rutgers M, van Pelt MJP, Dhert WJA, Creemers LB, Saris DBF. Evaluation of histological scoring systems for tissue-engineered, repaired and osteoarthritic cartilage. Osteoarthr Cartilage. 2010; 18(1):12–23.
23. Pritzker KPH, Gay S, Jimenez SA, Ostergaard K, Pelletier JP, Revell PA, Salter D, van den Berg WB. Osteoarthritis cartilage histopathology: grading and staging. Osteoarthr Cartilage. 2006; 14(1):13–29.
24. Custers RJH, Creemers LB, Verbout AJ, van Rijen MHP, Dhert WJA, Saris DBF. Reliability, reproducibility and variability of the traditional Histologic/Histochemical Grading System vs the new OARSI Osteoarthritis Cartilage Histopathology Assessment System. Osteoarthr Cartilage. 2007; 15(11):1241–1248.
25. Boskey A, Pleshko Camacho N. FT-IR imaging of native and tissue-engineered bone and cartilage. Biomaterials. 2007; 28(15):2465–2478. [PubMed: 17175021]
26. West PA, Bostrom MPG, Torzilli PA, Camacho NP. Fourier transform infrared spectral analysis of degenerative cartilage: An infrared fiber optic probe and imaging study. Appl Spectrosc. 2004; 58(4):376–381. [PubMed: 15104805]
27. Li GY, Thomson M, Dicarlo E, Yang X, Nestor B, Bostrom MPG, Camacho NP. A chemometric analysis for evaluation of early-stage cartilage degradation by infrared fiber-optic probe spectroscopy. Appl Spectrosc. 2005; 59(12):1527–1533. [PubMed: 16390593]
28. Hofmann GO, Marticke J, Grossstuck R, Hoffmann M, Lange M, Plettenberg HK, Braunschweig R, Schilling O, Kaden I, Spahn G. Detection and evaluation of initial cartilage pathology in man: A comparison between MRT, arthroscopy and near-infrared spectroscopy (NIR) in their relation to initial knee pain. Pathophysiology. 2010; 17(1):1–8. [PubMed: 19481428]
29. Marticke JK, Hosselbarth A, Hoffmeier KL, Marintschev I, Otto S, Lange M, Plettenberg HKW, Spahn G, Hofmann GO. How do visual, spectroscopic and biomechanical changes of cartilage correlate in osteoarthritic knee joints? Clin Biomech. 2010; 25(4):332–340.
30. Spahn G, Klinger HM, Baums M, Hoffmann M, Plettenberg H, Kroker A, Hofmann GO. Near-Infrared Spectroscopy for Arthroscopic Evaluation of Cartilage Lesions Results of a Blinded, Prospective, Interobserver Study. Am J Sports Med. 2010; 38(12):2516–2521. [PubMed: 20847221]

NIH-PA Author Manuscript NIH-PA Author Manuscript NIH-PA Author Manuscript


31. Spahn G, Plettenberg H, Kahl E, Klinger HM, Muckley T, Hofmann GO. Near-infrared (NIR) spectroscopy. A new method for arthroscopic evaluation of low grade degenerated cartilage lesions. Results of a pilot study. BMC Musculoskel Disord. 2007; 8:Article number 47.
32. Bellisola G, Sorio C. Infrared spectroscopy and microscopy in cancer research and diagnosis. Am J Cancer Res. 2012; 2(1):1–21. [PubMed: 22206042]
33. Siesler, HW. Basic Principles of Near-Infrared Spectroscopy. In: Ciurczak, EW.; Burns, DA., editors. Handbook of Near-Infrared Analysis. Boca Raton, FL, USA: CRC Press; 2007. p. 7-19.
34. Padalkar MV, Spencer RG, Nancy P. Near infrared spectroscopic evaluation of water in hyaline cartilage. Ann Biomed Eng. 201310.1007/s10439-013-0844-0
35. Spahn G, Plettenberg H, Nagel H, Kahl E, Klinger HM, Muckley T, Gunther M, Hofmann GO, Mollenhauer JA. Evaluation of cartilage defects with near-infrared spectroscopy (NIR): an ex vivo study. Med Eng Phys. 2008; 30(3):285–292. [PubMed: 17553725]
36. Hanh BD, Neubert RHH, Wartewig S, Christ A, Hentzsch C. Drug penetration as studied by noninvasive methods: Fourier transform infrared-attenuated total reflection, Fourier transform infrared, and ultraviolet photoacoustic spectroscopy. J Pharm Sci. 2000; 89(9):1106–1113. [PubMed: 10944375]
37. Faris F, Thorniley M, Wickramasinghe Y, Houston R, Rolfe P, Livera N, Spencer A. Noninvasive in vivo near-infrared optical measurement of the penetration depth in the neonatal head. Clin Phys Physiol Meas. 1991; 12(4):353–358. [PubMed: 1778034]
38. McCormick PW, Stewart M, Lewis G, Dujovny M, Ausman JI. Intracerebral penetration of infrared light. J Neurosurg. 1992; 76(2):315–318. [PubMed: 1730963]
39. Afara I, Prasadam I, Crawford R, Xiao Y, Oloyede A. Non-destructive evaluation of articular cartilage defects using near-infrared (NIR) spectroscopy in osteoarthritic rat models and its direct relation to Mankin score. Osteoarthr Cartilage. 2012; 20(11):1367–1373.
40. Afara I, Singh S, Oloyede A. Application of near infrared (NIR) spectroscopy for determining the thickness of articular cartilage. Med Eng Phys. 2013; 35(1):88–95. [PubMed: 22824725]
41. Afara IO, Prasadam I, Crawford R, Xiao Y, Oloyede A. Near infrared (NIR) absorption spectra correlates with subchondral bone micro-CT parameters in osteoarthritic rat models. Bone. 2013; 53(2):350–357. [PubMed: 23274676]
42. Brown CP, Bowden JC, Rintoul L, Meder R, Oloyede A, Crawford RW. Diffuse reflectance near infrared spectroscopy can distinguish normal from enzymatically digested cartilage. Phys Med Biol. 2009; 54(18):5579–5594. [PubMed: 19717892]
43. Brown CP, Jayadev C, Glyn-Jones S, Carr AJ, Murray DW, Price AJ, Gill HS. Characterization of early stage cartilage degradation using diffuse reflectance near infrared spectroscopy. Phys Med Biol. 2011; 56(7):2299–2307. [PubMed: 21411867]
44. Brown CP, Oloyede A, Crawford RW, Thomas GER, Price AJ, Gill HS. Acoustic, mechanical and near-infrared profiling of osteoarthritic progression in bovine joints. Phys Med Biol. 2012; 57(2): 547–559. [PubMed: 22217979]
45. Hanifi A, Bi XH, Yang X, Kavukcuoglu B, Lin PC, DiCarlo E, Spencer RG, Bostrom MPG, Pleshko N. Infrared Fiber Optic Probe Evaluation of Degenerative Cartilage Correlates to Histological Grading. Am J Sports Med. 2012; 40(12):2853–2861. [PubMed: 23108637]
46. Mankin H, Lippiell L, Dorfman H. Biochemical and metabolic changes in cartilage of femoral head in patients with osteoarthritis of hip. J Bone Joint Surg Am. 1970; A 52(3):606-&.
47. Mankin HJ, Dorfman H, Lippiell L, Zarins A. Biochemical and metabolic abnormalities in articular cartilage from osteo-arthritic human hips .2. correlation of morphology with biochemical and metabolic data. J Bone Joint Surg Am. 1971; A 53(3):523–537. [PubMed: 5580011]
48. Revelle, W. Procedures for Psychological, Psychometric, and Personality Research. Evanston, IL, USA: Northwestern University; 2013. http://CRAN.R-project.org/package=psych
49. R. D. C. Team. R: A language and environment for statistical computing. R Foundation for Statistical Computing. Vienna, Austria: 2012. http://www.R-project.org
50. Schneider CA, Rasband WS, Eliceiri KW. NIH Image to ImageJ: 25 years of image analysis. Nat Methods. 2012; 9(7):671–675. [PubMed: 22930834]
51. Osborne, BG.; Fearn, T.; Hindle, PH. Practical NIR spectroscopy with applications in food and beverage analysis. Harlow, UK: Longman Scientific & Technical; 1993.

NIH-PA Author Manuscript

NIH-PA Author Manuscript

NIH-PA Author Manuscript

52. Wold S, Sjostrom M, Eriksson L. PLS-regression: a basic tool of chemometrics. Chemometr Intell Lab Syst. 2001; 58(2):109–130.

53. Brennan P, Silman A. Statistical methods for assessing observer variability in clinical measures. Br Med J. 1992; 304(6840):1491–1494. [PubMed: 1611375]

54. Ateshian GA, Soslowsky LJ, Mow VC. Quantitation of articular surface topography and cartilage thickness in knee joints using stereophotogrammetry. J Biomech. 1991; 24(8):761–776. [PubMed: 1918099]

55. Johansson A, Kuiper JH, Sundqvist T, Persson F, Speier C, D'Alfonso D, Richardson JB, Oberg A. Spectroscopic Measurement of Cartilage Thickness in Arthroscopy: Ex Vivo Validation in Human Knee Condyles. Arthroscopy. 2012; 28(10):1513–1523. [PubMed: 22726814]

56. Oberg PA, Sundqvist T, Johansson A. Assessment of cartilage thickness utilising reflectance spectroscopy. Med Biol Eng Comput. 2004; 42(1):3–8. [PubMed: 14977216]

57. Kinnunen J, Saarakkala S, Hauta-Kasari M, Vahimaa P, Jurvelin JS. Optical spectral reflectance of human articular cartilage - relationships with tissue structure, composition and mechanical properties. Biomed Opt Express. 2011; 2(5):1394–1402. [PubMed: 21559150]

58. Johansson A, Sundqvist T, Kuiper JH, Oberg PA. A spectroscopic approach to imaging and quantification of cartilage lesions in human knee joints. Phys Med Biol. 2011; 56(6):1865–1878. [PubMed: 21364258]

NIH-PA Author Manuscript

NIH-PA Author Manuscript

NIH-PA Author Manuscript

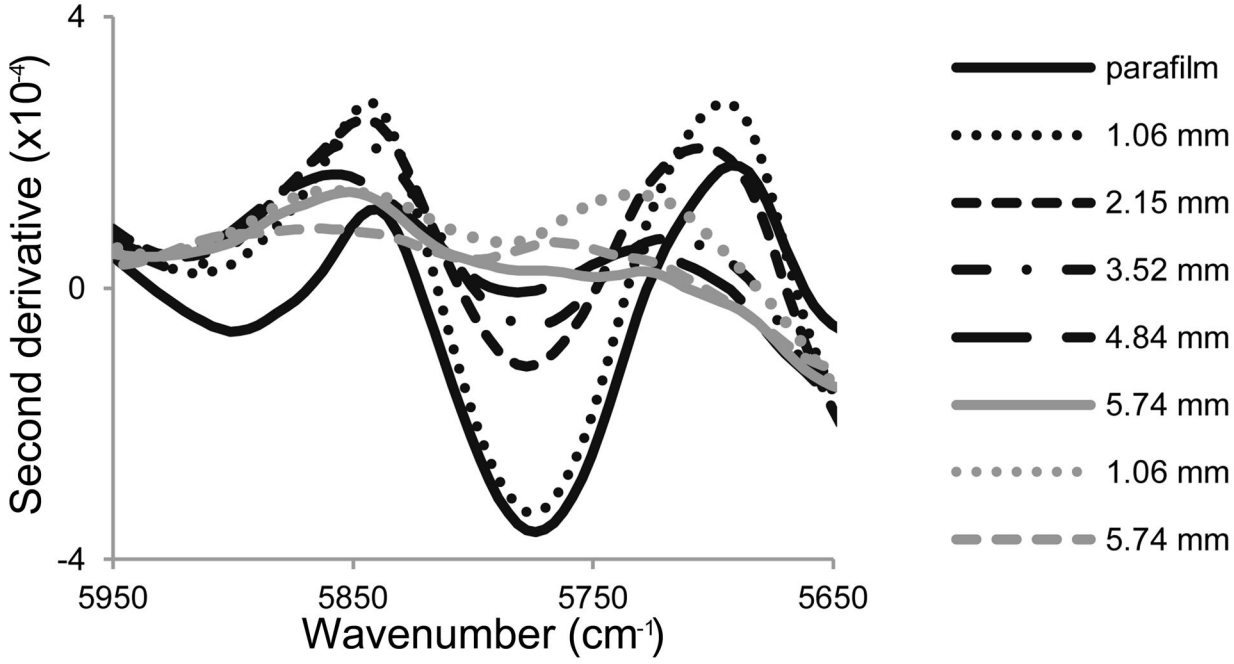


**Fig. 1.**

Second derivative (third order polynomial, 170 $cm^{-1}$ window) near infrared spectra of parafilm and cartilage sections of varying thickness, with (black spectra) and without (grey spectra) an underlying layer of parafilm. Evidence of parafilm was observed when the overlying layer of cartilage was less than 5 mm. The parafilm spectrum has been divided by a factor of 6 so that the 5774 $cm^{-1}$ peak is on the same scale.

NIH-PA Author Manuscript
NIH-PA Author Manuscript
NIH-PA Author Manuscript



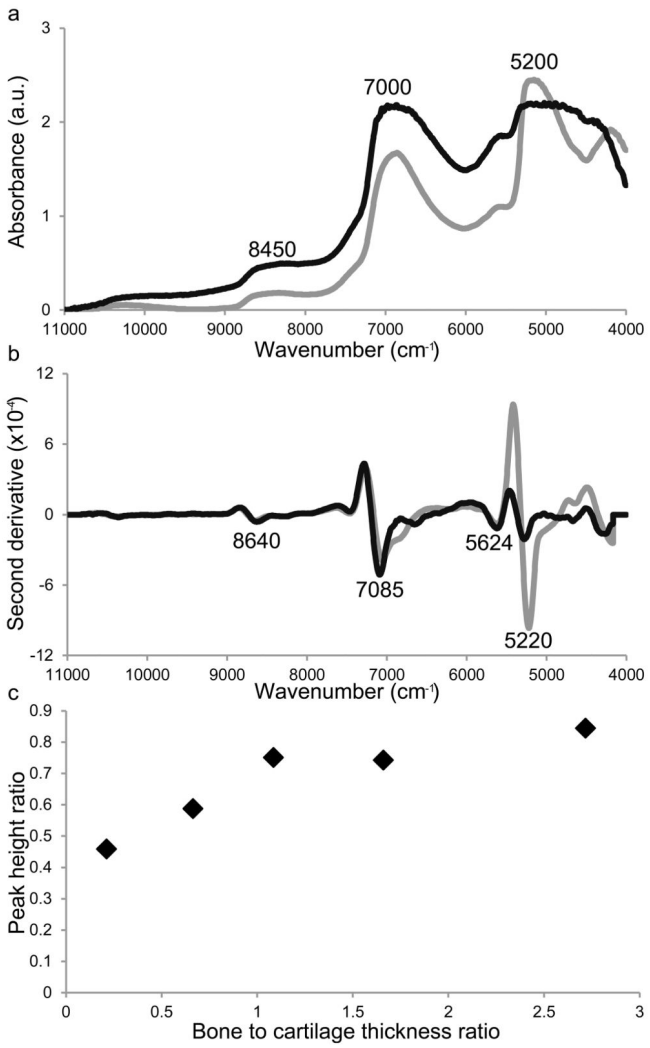


**Fig. 2.**

(a) Baseline offset corrected and (b) second spectra derivative (third order polynomial, 355 $cm^{-1}$ window) near infrared spectra of bone (grey) and cartilage (black). The NIR spectra were collected from bone and cartilage samples that were 3.56 and 3.52 mm thick respectively. (c) The peak height ratio of 5270 (free plus bound water) to 7085 $cm^{-1}$ (free water) as determined from the second derivative spectra of samples with varying amounts of bone and cartilage.

NIH-PA Author Manuscript

NIH-PA Author Manuscript

NIH-PA Author Manuscript

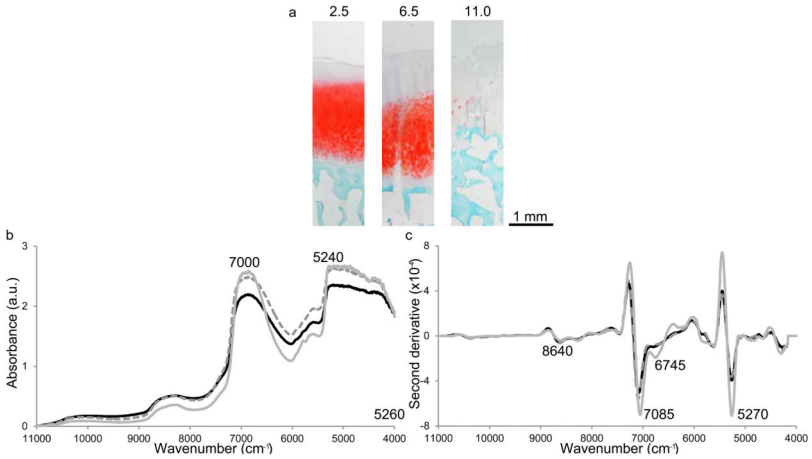


**Fig. 3.**

(a) Safranin-O sections, (b) baseline offset corrected and (c) second derivative (third order polynomial 355 $cm^{-1}$ window) near infrared spectra of samples with modified Mankin grades of 2.5 (black solid line), 6.5 (grey dashed line) and 11 (grey solid line; 2.30, 3.12 and 1.89 mm thick respectively). The spectra more closely resemble the spectrum of bone as Mankin grade increases.

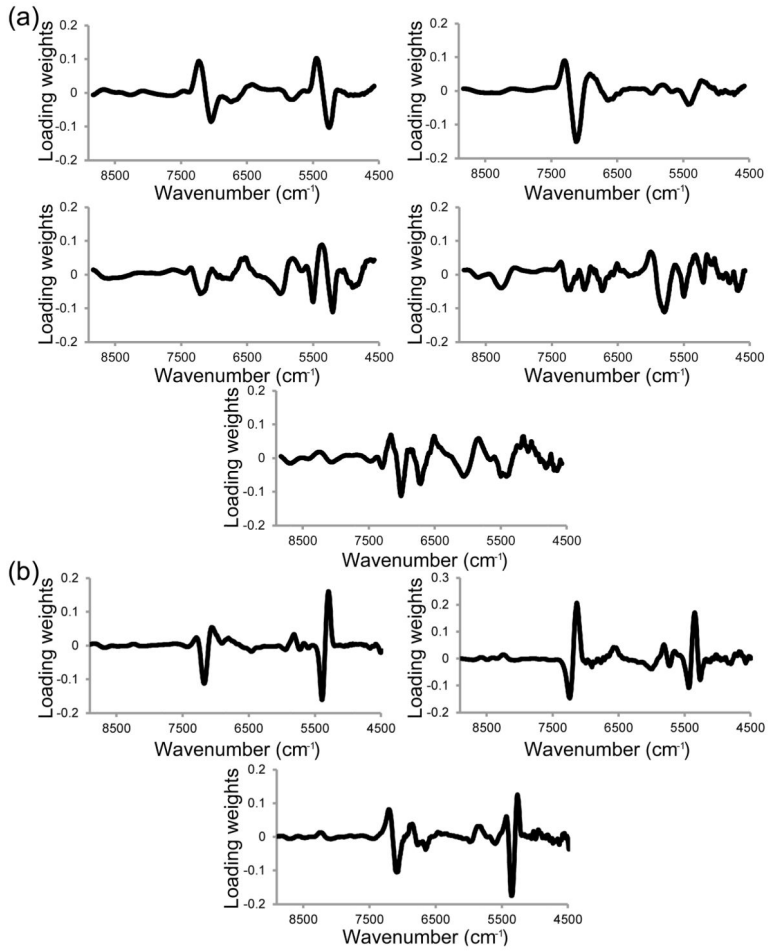


**Fig. 4.**

(a) First three factor loading weights of the cartilage thickness prediction model based on sample averaged 4400–9000 $cm^{-1}$ spectra that were pretreated with standard normal variate and second derivative (third order polynomial, 170 $cm^{-1}$ window) methods. (b) First five factor loading weights of the modified Mankin grade prediction model based on sample averaged 4400–9000 $cm^{-1}$ spectra that were pretreated with standard normal variate and second derivative (third order polynomial, 355 $cm^{-1}$ window) methods.



NIH-PA Author Manuscript NIH-PA Author Manuscript NIH-PA Author Manuscript

NIH-PA Author Manuscript

NIH-PA Author Manuscript

NIH-PA Author Manuscript

**Table I**

Modified Mankin scoring system

| | |
|---|---|
| Structure | |
| Normal | 0 |
| Surface irregularity | 1 |
| Clefts to transitional zone | 2 |
| Clefts to radial zone | 3 |
| Clefts to calcified zone | 4 |
| Complete disorganization | 5 |
| Cells | |
| Normal | 0 |
| Diffuse hypercellularity | 1 |
| Cloning | 2 |
| Tidemark integrity | |
| Normal/intact | 0 |
| Duplicated tidemark | 1 |
| Vascular invasion through first tidemark | 2 |
| Vascular invasion through second tidemark | 3 |
| Safranin O staining | |
| Normal | 0 |
| Slight reduction | 1 |
| Moderate reduction | 2 |
| Severe reduction | 3 |

NIH-PA Author Manuscript NIH-PA Author Manuscript NIH-PA Author Manuscript



**Table II**

Spearman correlation coefficients for cartilage thickness and Mankin grade with peak area and height parameters. Significant correlation coefficients ($P < 0.05$) are in bold.

| | Vibrational mode | Thickness | | Mankin grade | |
|---|---|---|---|---|---|
| **Peak area**[a] | | **R** | **P** | **R** | **P** |
| 7460–6780 $cm^{-1}$ | OH str. 1st OT[b] | **0.44**[c] | **0.02** | −0.30 | 0.08 |
| 8695–8197 $cm^{-1}$ | CH str. 2nd OT | **0.66** | **0.00** | **−0.54** | **0.00** |
| 8820–8060 $cm^{-1}$ | CH str. 2nd OT | **0.66** | **0.00** | **−0.56** | **0.00** |
| 7280–6040 $cm^{-1}$ | OH str. 1st OT | **0.40** | **0.03** | −0.30 | 0.08 |
| 5716–5496 $cm^{-1}$ | CH str. 1st OT | **0.50** | **0.01** | **−0.38** | **0.02** |
| Peak area ratio[a] | | | | | |
| 7460–6780/8695–8197 $cm^{-1}$ | OH str. 1st OT/CH str. 2nd OT | **−0.50** | **0.01** | **0.60** | **0.00** |
| 7280–6040/8820–8060 $cm^{-1}$ | OH str. 1st OT/CH str. 2nd OT | **−0.46** | **0.01** | **0.61** | **0.00** |
| 7280–6040/5716–5496 $cm^{-1}$ | OH str. 1st OT/CH str. 1st OT | **−0.57** | **0.00** | **0.42** | **0.01** |
| 8820–8060/5716–5496 $cm^{-1}$ | CH str. 2nd OT/CH str. 1st OT | 0.26 | 0.18 | **−0.59** | **0.00** |
| Peak height[d] | | | | | |
| 8640 $cm^{-1}$ | CH str. 2nd OT | **−0.73** | **0.00** | 0.21 | 0.22 |
| 8266 $cm^{-1}$ | CH str. 2nd OT | **0.52** | **0.00** | −0.28 | 0.11 |
| 6418 $cm^{-1}$ | NH str. 1st OT | **−0.47** | **0.01** | 0.15 | 0.37 |
| 6025 $cm^{-1}$ | CH str. 1st OT | **−0.62** | **0.00** | 0.23 | 0.18 |
| 5824 $cm^{-1}$ | CH str. 1st OT | **0.70** | **0.00** | −0.16 | 0.36 |
| Minimum peak height[d] | | | | | |
| 5353–5153 $cm^{-1}$ | | **0.65** | **0.00** | −0.27 | 0.12 |
| 7201–7000 $cm^{-1}$ | OH str. 1st OT | 0.29 | 0.12 | **−0.60** | **0.00** |
| 8755–8500 $cm^{-1}$ | CH str. 2nd OT | **−0.72** | **0.00** | 0.21 | 0.24 |
| Minimum peak height ratio[d] | | | | | |

NIH-PA Author Manuscript
NIH-PA Author Manuscript
NIH-PA Author Manuscript



| | Vibrational mode | Thickness | | Mankin grade | |
|---|---|---|---|---|---|
| **Peak area**[a] | | **R** | **P** | **R** | **P** |
| 5353–5153/7201–7000 $cm^{-1}$ | OH combinations/OH str. 1st OT | **−0.52** | **0.00** | 0.13 | 0.46 |
| 5353–5153/8755–8500 $cm^{-1}$ | OH combinations/CH str. 2nd OT | **−0.68** | **0.00** | 0.25 | 0.15 |
| 7201–7000/8755–8500 $cm^{-1}$ | OH str. 1st OT/CH str. 2nd OT | **−0.75** | **0.00** | 0.36 | 0.03 |
| Peak position[d] | | | | | |
| 5353–5153 $cm^{-1}$ | OH combinations | **0.43** | **0.02** | −0.16 | 0.36 |
| 7201–7000 $cm^{-1}$ | OH str. 1st OT | **0.52** | **0.00** | −0.13 | 0.46 |
| 8755–8500 $cm^{-1}$ | CH str. 2nd OT | **0.62** | **0.00** | **−0.41** | **0.02** |

[a] These parameters were calculated from baseline offset corrected spectra.

[b] str. – stretching, OT – overtone.

[c] Values in bold are statistically significant.

[d] These parameters were calculated from second derivative (Savitzky-Golay 3rd order polynomial, 339 $cm^{-1}$ window).